Effect of Moving Surfaces on the Airfoil Boundary-Layer Control

V. J. Modi* and F. Mokhtarian†
University of British Columbia, Vancouver, B.C., Canada
and
T. Yokomizo
Kanto Gakuin University, Yokohama, Japan

The concept of moving surface boundary-layer control, as applied to a Joukowsky airfoil, is investigated through a planned experimental program complemented by a flow visualization study. The moving surface was provided by rotating cylinders located at the leading and trailing edges of the airfoil. The leading-edge rotating cylinder extends the lift curve without substantially affecting its slope, thus effectively increasing the maximum lift and delaying stall. In general, the performance improves with an increase in the ratio of cylinder surface speed U_c to the freestream speed U. A rotating trailing-edge cylinder affects the airfoil characteristics in a fundamentally different manner. It acts as a flap and shifts the C_L vs α curves to the left, thus increasing the lift coefficients before stall. For example, at $\alpha = 4$ deg, it increased the C_L by about 320%. In conjunction with the leading-edge cylinder, it can provide significant improvements in lift over the entire range of small to moderately high angles of incidence ($\alpha \leq 18$ deg). A flow visualization study substantiates, rather spectacularly, effectiveness of the concept.

Introduction

EVER since the introduction of the boundary-layer concept by Prandtl, there has been a constant challenge faced by scientists and engineers to minimize its adverse effects and control it to an advantage. Methods such as suction, blowing, vortex generators, turbulence promoters, etc., have been investigated at length and employed in practice with a varying degree of success. A vast body of literature accumulated over the years has been reviewed rather effectively by several authors including Goldstein,[1] Lachmann,[2] Rosenhead,[3] Schlichting,[4] and Chang,[5] among others. However, the use of moving wall for boundary-layer control has received relatively little attention.

Irrespective of the method used, the main objective of a control procedure is to prevent or at least delay the separation of boundary layer from the wall. A moving surface attempts to accomplish this in two ways: 1) by retarding the initial growth of the boundary layer through reduction in relative motion between the surface and the free stream, and 2) by injecting momentum into the existing boundary layer.

The most practical application of moving wall for boundary-layer control was demonstrated by Favre.[6] Using an airfoil with an upper surface formed by a belt moving over two rollers, he was able to delay separation until the angle of attack reached 55 deg, where the maximum lift coefficient of 3.5 was realized. Alvarez-Calderon and Arnold[7] carried out tests on a rotating cylinder flap to evolve a high-lift airfoil for STOL-type aircraft. The system was flight tested on a single-engine, high-wing research aircraft designed by the Aeronautics Division of the Universidad Nacional de Ingenieria in Lima, Peru.[8]

Of some interest is the North American Rockwell designed OV-10A aircraft, which was flight tested by NASA's Ames Research Center.[9-11] Cylinders, located at the leading edges of the flaps, were rotated at high speed with the flaps in lowered position. The main objective of the test program was to assess handling qualities of the propeller-powered STOL type aircraft at higher lift coefficients. The aircraft was flown at speeds of 29–31 m/s, along approaches up to −8 deg, which corresponded to a lift coefficient of about 4.3. In the pilot's opinion, any further reductions in approach speed were limited by the lateral-directional stability and control characteristics. Excellent photographs of the airplane on ground (showing the cylinders in position) and in flight have been published in *Aviation Week and Space Technology*.[12]

Efforts thus far, though useful to an extent, were generally aimed at specific configurations and lacked an approach to the problem at a fundamental level and in an organized fashion. From this point of view, Tennant's contribution to the field is significant. Tennant et al.[13] have conducted tests with a wedge shaped flap having a rotating cylinder as the leading edge. Flap deflection was limited to 15 deg and the critical cylinder velocity necessary to suppress separation was determined. Effects of increase in gap size (between the cylinder and the flap surface) were also assessed. No effort was made to observe the influence of an increase in cylinder surface velocity beyond $U_c/U = 1.2$. More recently, Tennant et al.[14] have reported circulation control for a symmetrical airfoil with a rotating cylinder forming its trailing edge. For zero angle of attack, a lift coefficient of 1.2 was attained with $U_c/U = 3$. Also of interest are Tennant et al.'s studies concerning the boundary-layer growth on moving surfaces accounting for gap effects.[15,16]

With reference to V/STOL application, the preliminary experimental study by Modi et al.[17] with NACA 63-218 (modified) airfoil used in the Canadair CL-84 is relevant. The test program involved models with or without a plain slotted flap. The objective was to assess influence of the rotating cylinders at the leading edge of the flap in conjunction with that at the leading edge of the airfoil. In general, the rear cylinder did not contribute substantially to the improvement in performance, at least in the configuration tested. In fact, in

Presented as Paper 88-4337 at the AIAA Atmospheric Flight Mechanics Conference, Minneapolis, MN, Aug. 15–17, 1988; received Aug. 31, 1988; revision received Feb. 17, 1989.

*Professor, Department of Mechanical Engineering. Associate Fellow AIAA.
†Graduate Research Assistant; presently Staff Engineer, Canadair Ltd., Montreal.
‡Professor, Department of Mechanical Engineering.

certain situations, due to presence of an additional gap, it affected the performance adversely. More recently, the authors studied the problem numerically using the surface singularity method, and confirmed its effectiveness through detailed experimental measurements.[18] The predicted pressure distributions were found to be in good agreement with the experimental data almost up to the point of complete separation from the airfoil surface, except near the trailing edge.

The investigation reported here builds upon this body of literature. It studies fluid dynamics of an airfoil with the moving surface boundary-layer control using an extensive wind tunnel test program. The experimental study uses a multisection symmetrical Joukowsky model, which allows the use of one or more rotating cylinders at various locations around the airfoil. An extensive flow visualization study complements the experimental results.

Wind Tunnel Test Program

The wind tunnel model, a symmetrical Joukowsky airfoil of 15% maximum thickness to chord ratio, approximately 0.38 m along chord and 0.68 m long, spanned the tunnel test section 0.91 × 0.68 × 2.6 m to create an essentially two-dimensional condition. The model was provided with pressure taps, suitably distributed over the circumference, to yield detailed information concerning the surface loading. It was supported by an Aerolab six component strain gauge balance and tested in a low-speed, low-turbulence, return-type wind tunnel where the air speed can be varied from 1–50 m/s with a turbulence level of less than 0.1%. A Betz micromanometer with an accuracy of 0.2 mm of water was used to measure pressure differential across the contraction section of 7:1 ratio. The rectangular test section (0.91 × 0.68 m) is provided with 45 deg corner fillets that vary from 15.25 × 15.25 to 12 × 12 cm to partly compensate for the boundary-layer growth. The spatial variation of velocity in the test section is less than 0.25%.

To provide flexibility in locating the cylinder on the airfoil and permit testing of multicylinder configurations, a sectional design was adopted. The model consists of an aluminum skin wrapped around an aluminum and steel frame with various sections of the surface removable, as required, to accommodate cylinders.

The rotating cylinders were mounted between high-speed bearings, housed in the brackets at either end of the model. They were driven by 1/4 hp, 3.8 A variable speed motors, located outside the tunnel, through a standard coupling (Fig. 1). Three different configurations were tested: the airfoil with a rotating cylinder at the leading edge, trailing edge, and both edges.

The model was provided with a total of 44 pressure taps, distributed over the circumference, to yield detailed information about the surface loading. However, once a section of the model was removed to accommodate a cylinder, the pressure taps in that section were lost. Although the pressure information over the small region represented by the upper-cylinder is not of particular significance, the corresponding data at the leading edge of the airfoil is crucial, since it represents a high suction region. Its measurement represented a challenging task. Locating pressure taps on the surface of the cylinder, typically rotating in the range of 2000 to 7000 rpm offers considerable practical difficulty. The problem was resolved by measuring the pressure in the immediate vicinity of the cylinder rather than on the surface itself.

This was achieved by keeping the pressure taps stationary while the cylinder rotated. By locating the tap in a narrow ring, the width of which represented only a very small fraction of that of the cylinder, it was possible to ensure the continuity of flow over the entire surface and obtain an estimate of the surrounding pressure. The leading-edge cylinder was provided with a groove to house the "pressure rings" while maintaining the cylinder surface uniform. Figure 2 shows details of the leading-edge geometry and position of the pressure taps.

The tests were conducted over an extended range of angles of attack and cylinder rotational speeds, corresponding to $U_c/U = 0, 1, 2, 3, 4$, at a Reynolds number of 4.62×10^4. The choice of the Reynolds number in this case was dictated by

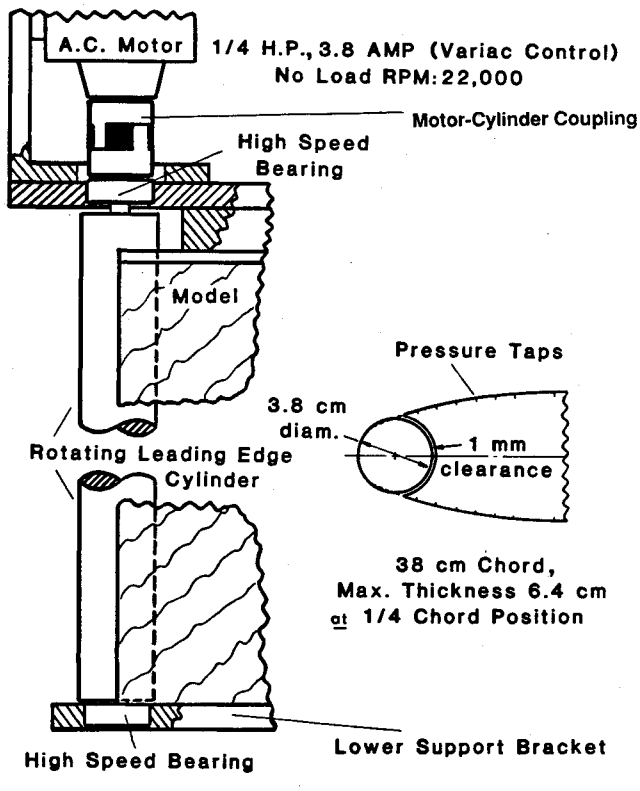

Fig. 1 Detailed schematic of the leading-edge rotating cylinder and cylinder-drive mechanism.

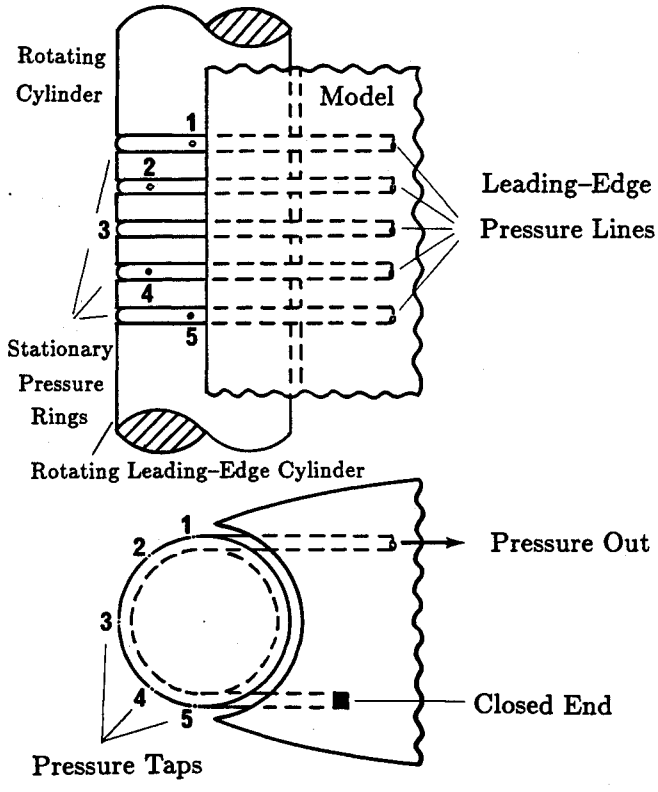

Fig. 2 Schematic diagram of the leading-edge construction of the Joukowsky model showing the details of the pressure taps.

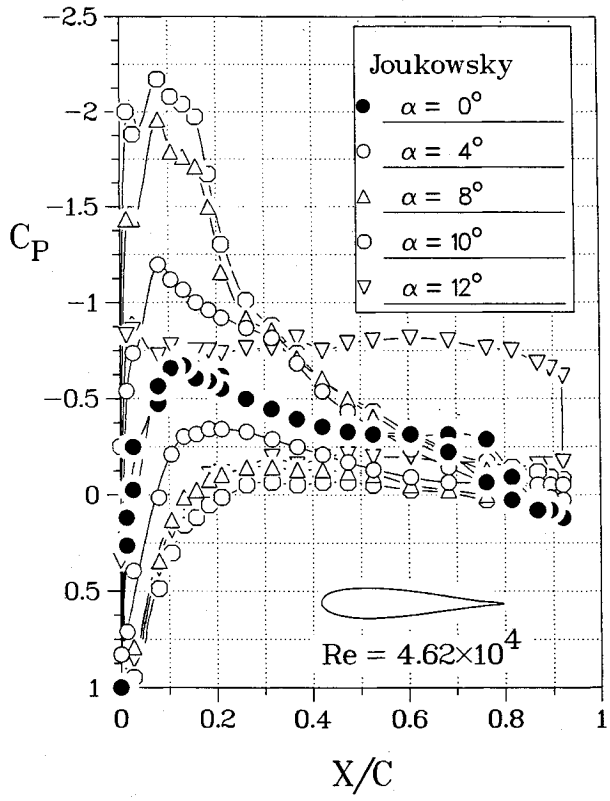

Fig. 3 Experimentally obtained pressure distributions for the basic Joukowsky model.

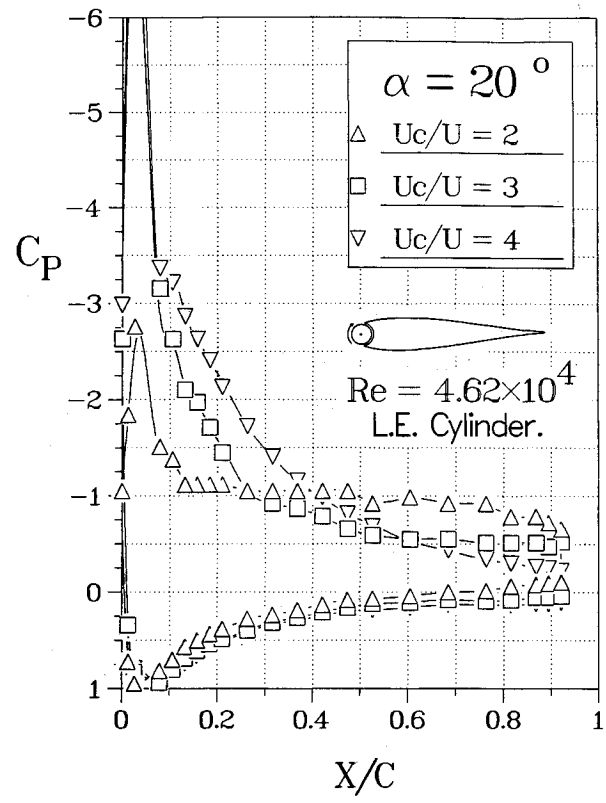

Fig. 5 Effect of increasing the rate of cylinder rotation on pressure distribution around the model at a relatively large angle of attack of 20 deg.

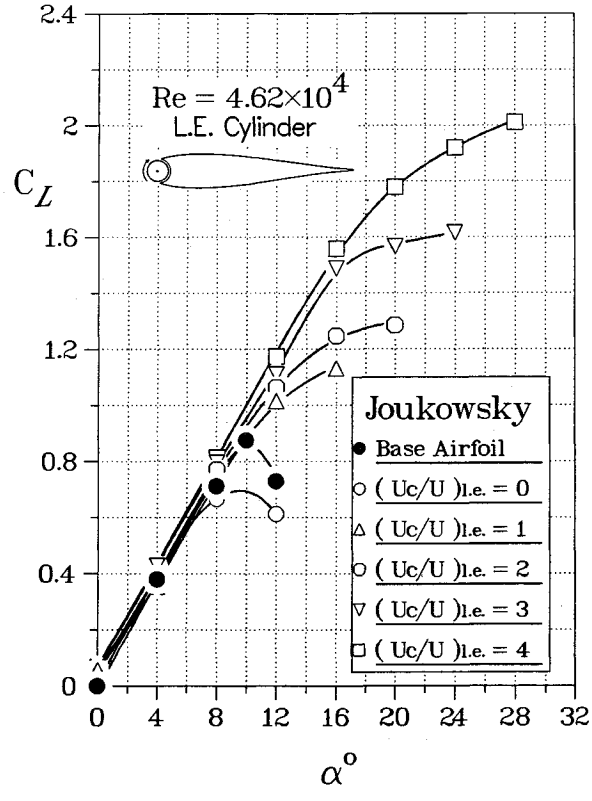

Fig. 4 Effect of the leading-edge cylinder rotation on the lift and stall characteristics of the Joukowsky model.

vibration problems with multicylinder configurations operating at high rotational speeds. The pressure plots were integrated in each case to obtain the lift coefficient. The lift was also measured independently using a strain gauge balance to assess the two-dimensional character of the test arrangement.

Results and Discussion

The relatively large angles of attack used in the experiments result in a considerable blockage of the wind tunnel test section, from 21% at $\alpha = 30$ deg to 30% at $\alpha = 45$ deg. The wall confinement leads to an increase in local wind speed, at the location of the model, thus resulting in an increase in aerodynamic forces. Several approximate correction procedures have been reported in literature to account for this effect. However, these procedures are mostly applicable to streamlined bodies with attached flow. A satisfactory procedure applicable to bluff bodies with large blockage is still not available.

With rotation of the cylinder(s), the problem is further complicated. As shown by the pressure data and confirmed by the flow visualization, the unsteady flow can be separating and reattaching over a large portion of the top surface. In absence of any reliable procedure to account for wall confinement effects in the present situation, the results are purposely presented in the uncorrected form.

The pressure distribution data for the "base airfoil" (in absence of the modifications imposed by the leading and trailing edge cylinders) are presented in Fig. 3. The leading edge was now formed by a snugly fitting plug. These results serve as a reference to assess the effect of rotating cylinders in different locations.

Figure 4 summarizes the effects of modification of the airfoil with the leading-edge cylinder and the cylinder rotation. The base airfoil has a maximum lift coefficient of about 0.87 at an angle of attack of 10 deg. There is a penalty

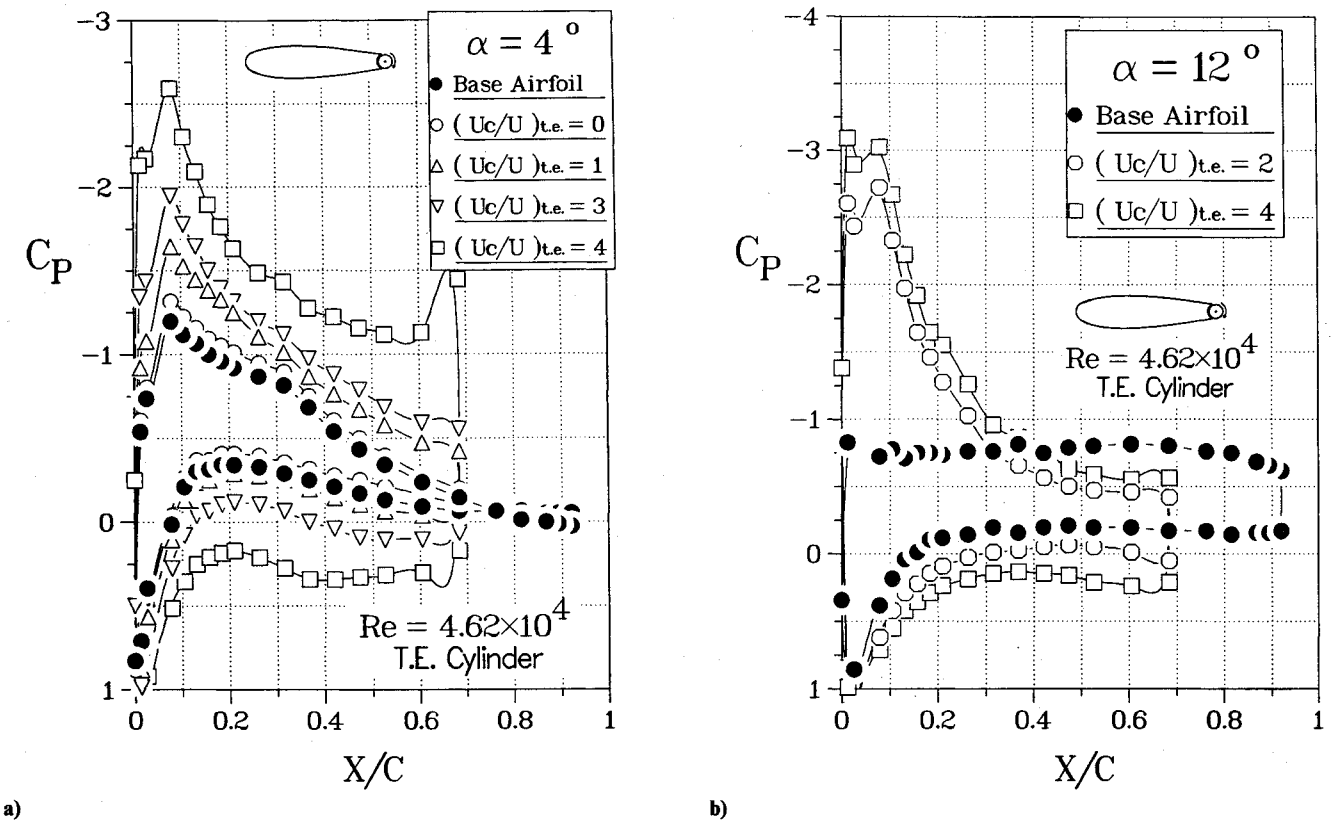

a) b)

Fig. 6 Pressure distributions over the Joukowsky model modified with a trailing-edge cylinder.

associated with the modified nose geometry, as well as due to the gap, but even at the lowest rate of rotation of the cylinder ($U_c/U = 1$), the lift and stall characteristics are significantly improved. The airfoil exhibits a desirable flattening of the lift curve at stall. The maximum lift coefficient measured with $U_c/U = 4$ was around 2.0 at $\alpha = 28$ deg, which is almost 2.3 times the lift coefficient of the base airfoil.

Selected pressure plots at relatively larger angles are presented in Fig. 5 to assist in more careful examination of the local flowfield. As the angle of attack of the airfoil is increased, the flow starts to separate from the upper surface closer to the leading edge. At $\alpha = 20$ deg, for example, the cylinder rotating at $U_c/U = 1$ kept the flow attached only near the leading edge. As the rate of rotation is increased, however, the size of the separation region is reduced and at the higher rates of rotation, the flow is again completely attached. The flow separates at around $X/C = 15\%$ with $U_c/U = 2$, around $X/C = 50\%$ when U_c/U is increased to 3, and at the trailing edge with the highest U_c/U used. The flow visualization study discussed later substantiated this general behavior rather dramatically.

The model was next tested with the trailing-edge cylinder. Unlike the leading-edge configuration, the cylinder at the trailing edge changes the basic geometry substantially. The trailing edge of the airfoil beyond $\approx 72\%$ chord is removed to accommodate the cylinder. The resulting chord is approximately 28% shorter than that of the base airfoil, and the model has a blunt trailing edge in the form of a cylinder.

Only a representative set of pressure plots for this model are presented in Fig. 6. In absence of the cylinder rotation, the pressure distribution over the airfoil is not changed substantially compared to that for the model with the trailing edge. With rotation of the trailing-edge cylinder, both the suction over the upper surface and the compression on the lower surface increase. The effect is particularly noticeable with the higher rate of cylinder rotation and at the lower angles of attack (Fig. 6a). The relative improvement decreases at the

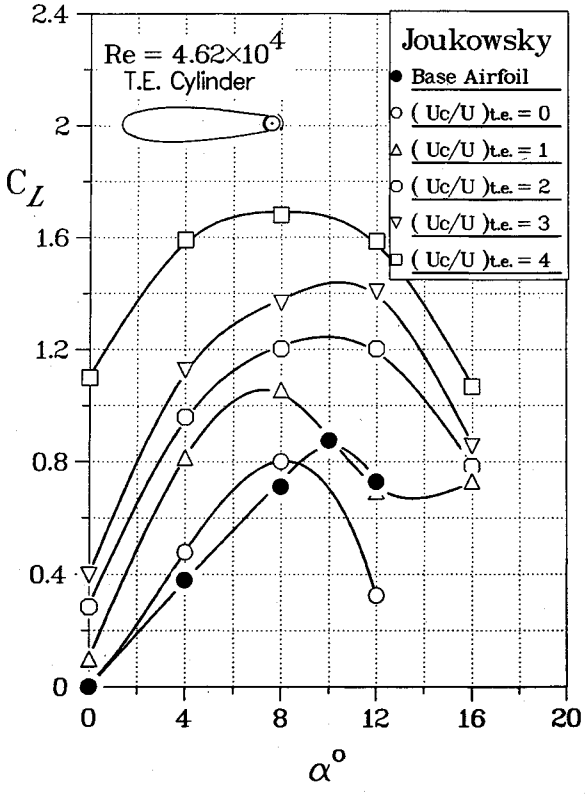

Fig. 7 Effect of the trailing-edge cylinder rotation on the lift and stall characteristics of the Joukowsky model.

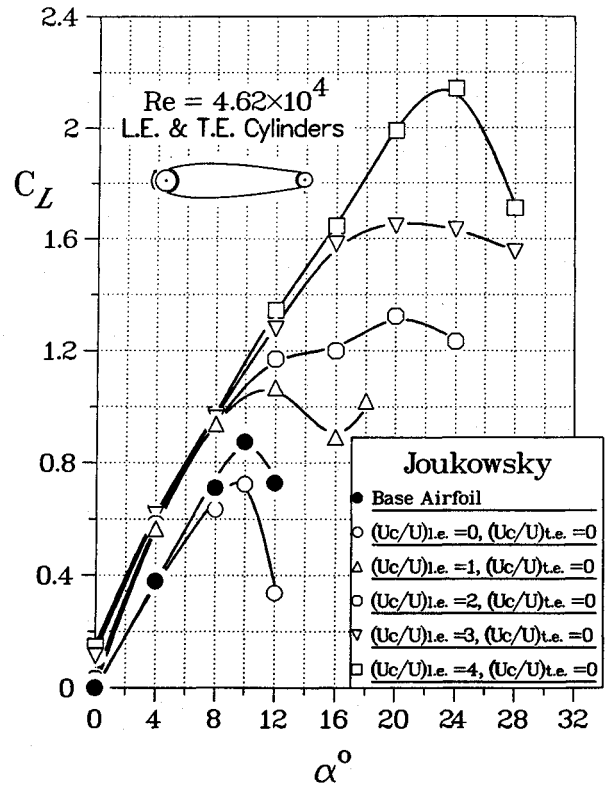

a) Leading-edge cylinder rotation

larger angles but is still quite evident at and beyond the stall (Fig. 6b).

This, in turn, results in a large improvement in the lift coefficient, as shown in Fig. 7. For example, rotating the trailing-edge cylinder at $U_c/U = 4$ results in an increase in lift by about 320% at $\alpha = 4$ deg (about 130% at $\alpha = 8$ deg). In contrast to the leading-edge cylinder, however, this configuration does not extend the stall beyond that of the base configuration. As can be expected, the trailing-edge cylinder essentially behaves as a flap shifting the plots to the left.

The use of a leading-edge cylinder extends the lift curve, thus substantially increasing the maximum lift coefficient and delaying stall. On the other hand, the trailing-edge cylinder rotation results in an improvement in the lift coefficient, at a given angle of attack, before stall. In order to combine these effects, the base configuration was modified to include both the leading- and trailing-edge cylinders. This phase of the test program examines the effect of individual and combined cylinder rotations.

The effect of rotating the leading-edge cylinder while the trailing-edge cylinder is stationary is summarized in Fig. 8a. The leading-edge cylinder rotation still appears to be quite effective in improving the lift and stall characteristics of the base configuration, although presence of the trailing-edge cylinder introduces an additional gap. The $C_{L,\max}$ shows a slight increase compared to the sharp trailing-edge case (2.15 vs 2, Fig. 4), which reflects the combined effect of the trailing-edge cylinder gap and a reduction in the chord. However, due to the modified nose geometry and the presence of a gap associated with the use of a leading-edge cylinder, performance of the trailing-edge cylinder itself is also affected. Although Fig. 8b shows a significant increase in $C_{L,\max}$ as a result of the trailing-edge cylinder rotation, the improvement is considerably less than that obtained previously (Fig. 7).

It is, however, the combined effects of both the cylinders that is of interest here. The results shown in Fig. 8c suggest

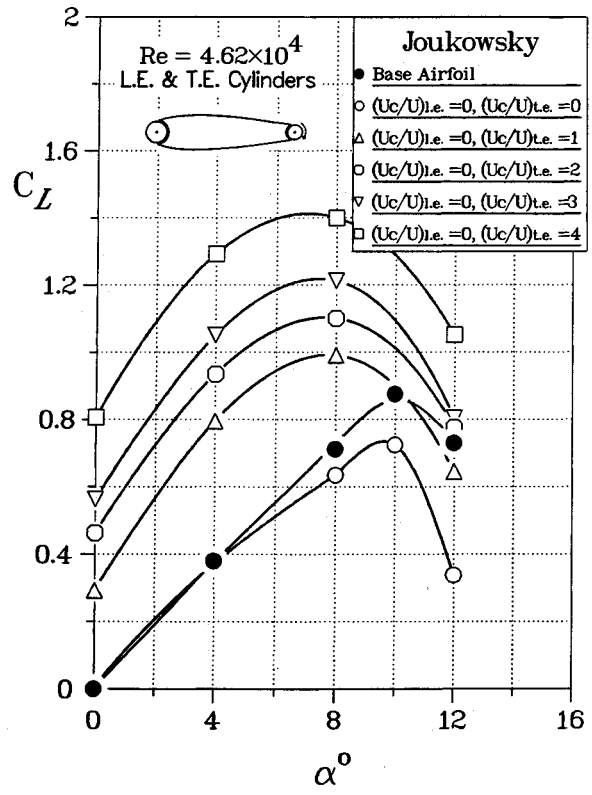

b) Trailing-edge cylinder rotation

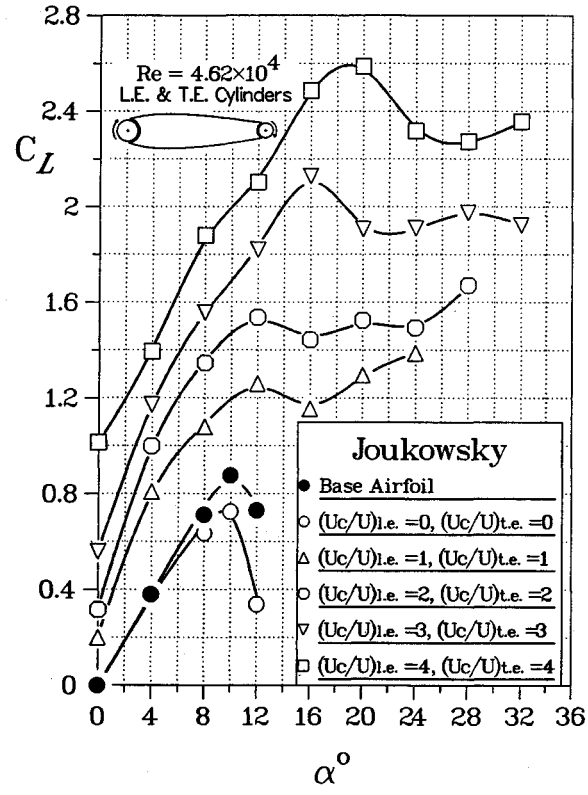

c) Combined rotation of both the cylinders

Fig. 8 Variation of C_L vs α for a modified Joukowsky airfoil with leading- and trailing-edge cylinders.

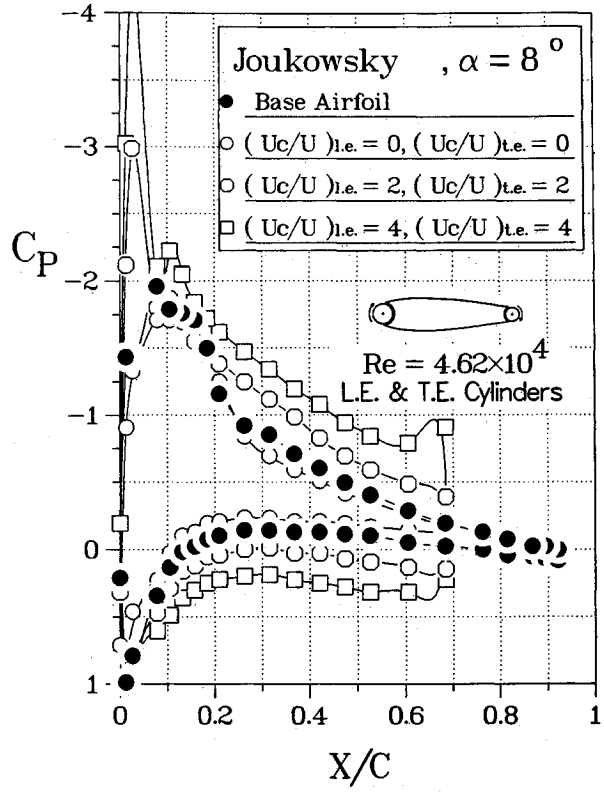

Fig. 9 Selected pressure plots for the Joukowsky model, modified with leading- and trailing-edge cylinders at $\alpha = 8$ deg.

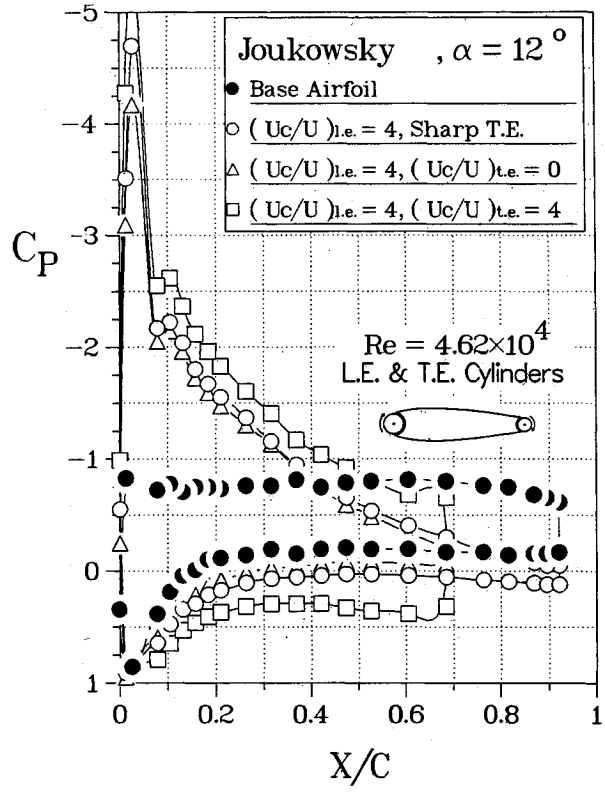

a)

some benefit due to rotation of the two cylinders together. Although the increase in $C_{L,\max}$ is rather modest (from 2.0 to 2.5, around 30%) compared to the leading-edge cylinder case (sharp trailing edge, Fig. 4), the lift coefficient at a given α is indeed increased significantly, as expected, due to the leftward shift of the plots (compare Figs. 8a and 8c). As noted before, this is due to the added circulation contributed by the trailing-edge cylinder. For example, $C_L = 0.8$ at $\alpha = 8$ deg and $(U_c/U)_{t.e.} = 3$ (Fig. 4), whereas for the same angle of attack and $(U_c/U)_{t.e.} = (U_c/U)_{t.e.} = 3$ the corresponding $C_L \approx 1.57$, an increase of around 96%. Similarly, $C_L \approx 1.55$ for $\alpha = 16$ deg and $(U_c/U)_{t.e.} = 4$. On the other hand, with both the cylinders rotating at $U_c/U = 4$, the lift coefficient is around 2.48, a further gain of about 60%. Note the maximum life coefficient attained with rotation of both cylinders represents an increase of 195% with respect to the reference configuration ($C_{L,\max}$ of about 2.6 vs 0.88, Fig. 8c).

A typical set of corresponding pressure plots are given in Fig. 9. At $\alpha = 8$ deg, a substantial increase in lift with cylinder rotation is quite evident. The suction peak over the leading edge associated with the rotation of the leading-edge cylinder, as well as an increase in suction over the upper surface and in compression on the lower surface due to rotation of the trailing-edge cylinder, can be observed quite clearly.

The pressure data are also compared with those for the leading-edge cylinder configuration, with and without the sharp trailing edge, in Fig. 10. At $\alpha = 12$ deg (Fig. 10a), the adverse effect of replacing the sharp trailing edge with a cylinder is still quite small and rotation of the trailing-edge cylinder results in an increased lift. The penalty becomes more evident, however, as the angle of attack is further increased. The rotation of the cylinder becomes less effective, and at $\alpha = 24$ deg the flow separates earlier than that in the leading-edge cylinder case (Fig. 10b). Thus, the higher lift coefficients obtained, at low to moderately high angles of attack, are at the cost of the lower maximum lift coefficient and stall angle.

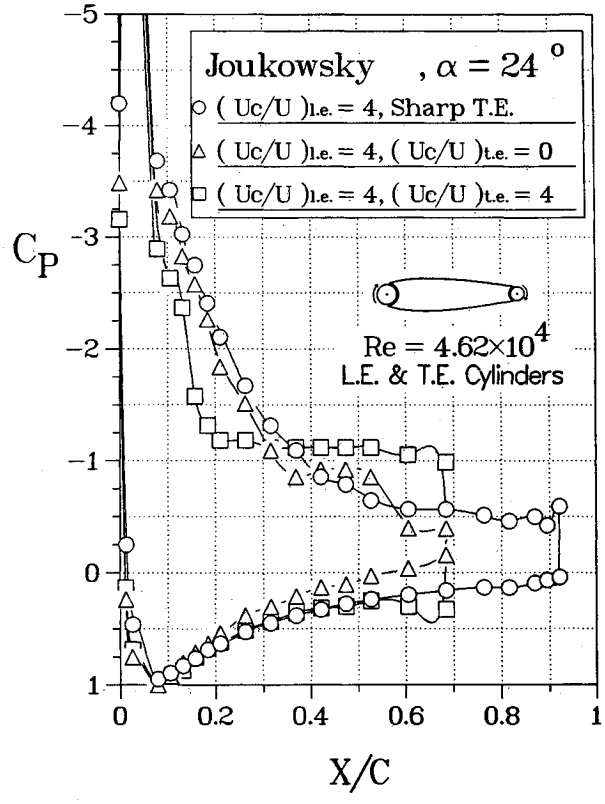

b)

Fig. 10 Comparison of pressure plots for the model with several combinations of leading- and trailing-edge cylinder configurations.

To better appreciate the overall effect of this twin cylinder configuration, the results are summarized in Fig. 11. The base data correspond to the model with the leading-edge fill-in section (no gap) and the sharp trailing edge. Modifying the configuration with the leading- and trailing-edge cylinders adversely affects the $C_{L,\max}$, which now reduces from around 0.88 to ≈ 0.73. The trailing-edge cylinder rotating at $(U_c/U)_{t.e.} = 4$ not only makes up for the loss but actually increases C_L, particularly at $\alpha \leq 8$ deg. However, the stall angle is reduced from around 10 to 8 deg due to leftward movement of the curve caused by an increase in circulation. The leading edge cylinder rotating at $(U_c/U)_{l.e.} = 4$, with the trailing-edge cylinder stationary, significantly increases the $C_{L,\max}$ to around 2.13 with the stall delayed to 24 deg, an increase of about 140% with respect to the base configuration ($\approx 192\%$ with reference to the modified configuration). With both the cylinders rotating at $U_c/U = 4$, there is a further increase in $C_{L,\max}$ and a substantial increase in lift for $\alpha \leq 19$ deg, the new stall angle.

Note the C_L values for this leading and trailing-edge twin cylinder case are much higher than those given by the leading-edge cylinder at lower angles of attack (Fig. 4). The α_{stall} for this configuration, which is now around 19 deg, is still lower than the corresponding stall angle of the leading-edge cylinder alone with the sharp trailing edge.

One would like to assess relative merit of the moving surface boundary-layer control with other procedures for generating high lift, such as blowing, suction, etc. Obviously, to be useful, such a comparison has to be based on well-planned experiments conducted under controlled and comparable conditions, as otherwise it can lead to misleading conclusions. Unfortunately, such results permitting rational comparison have not been recorded in the literature. However, it is possible to make a few general observations.

Besides its striking success in increasing lift and delaying stall, one of the attractive features of moving surface boundary-layer control is the negligible amount of power

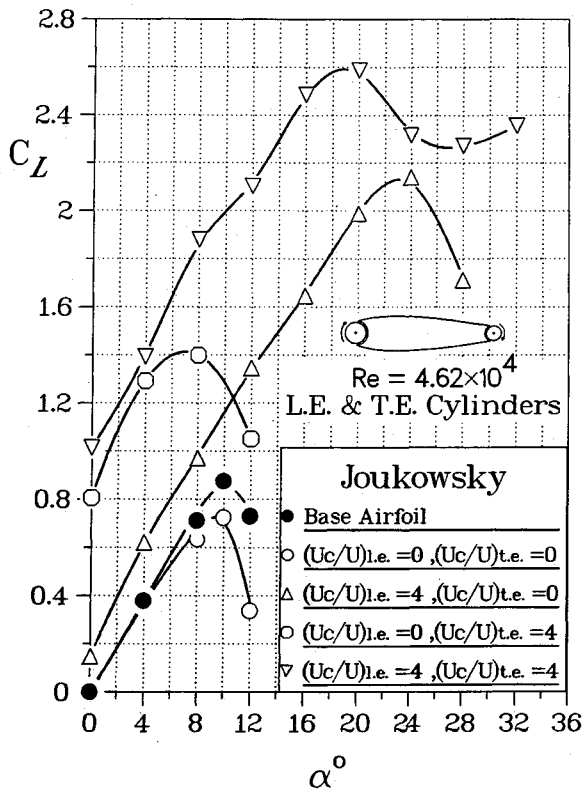

Fig. 11 Effect of rotation of the leading- and trailing-edge cylinders on the lift and stall characteristics of the Joukowsky airfoil model.

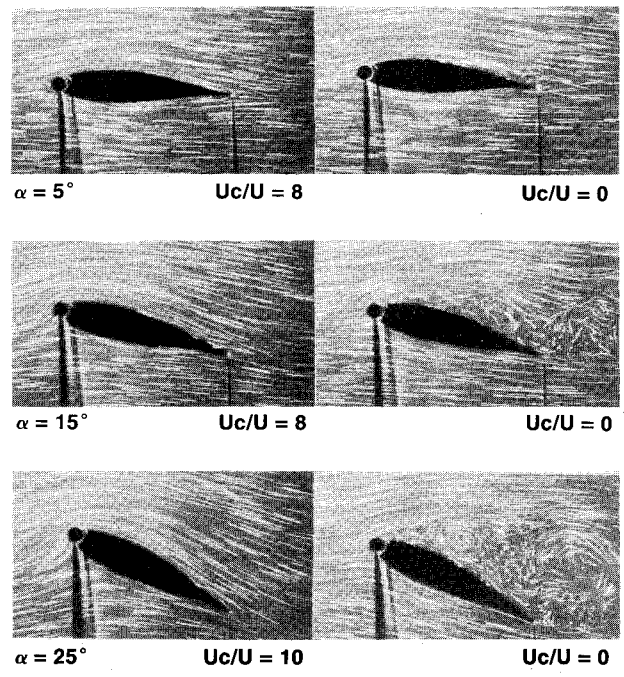

Fig. 12 Flow visualization photographs showing the steady flow over the airfoil at various angles of attack with and without the rotation of the leading edge.

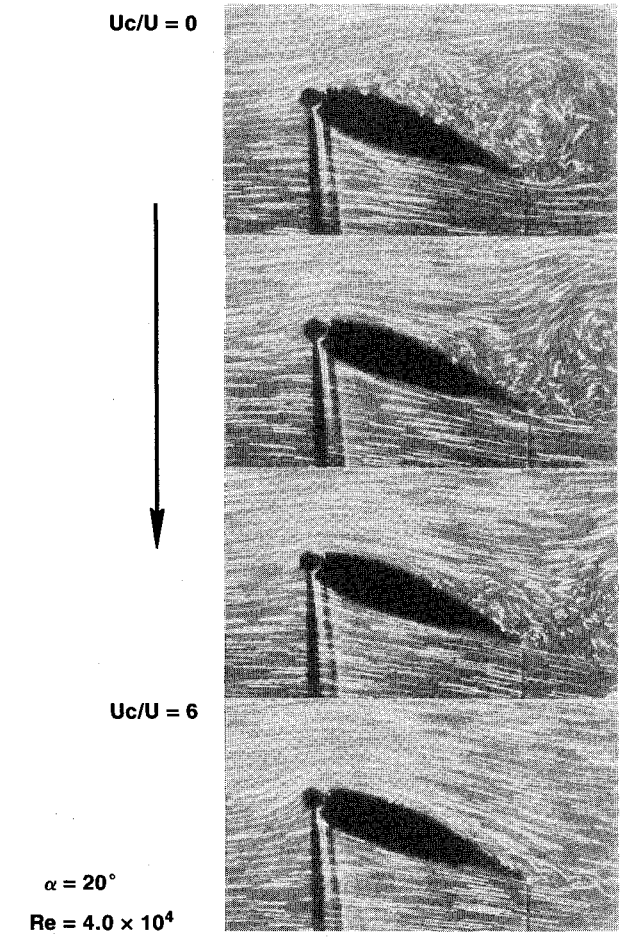

Fig. 13 Flow visualization photographs showing the transition from the highly separated flow in the absence of cylinder rotation to the essentially reattached flow at $U_c/U = 6$.

involved in driving the cylinders. Essentially, it corresponds to the bearing friction and the torque contributed by the forces on the surface of the cylinder. Note the cylinders themselves can be hollow, thus minimizing the inertia effect. The 1/4 hp motor used in the present study was much larger than necessary, and was used because of availability. Even a 1/16 hp motor would have served the purpose. Thus, the power required is virtually insignificant compared to active blowing or suction for boundary-layer control, where the power consumption is likely to be considerably larger.

It is also of interest to recognize that the trailing-edge cylinder increases the lift primarily through circulation control. Thus, it has some similarity with the conventional flap, as well as the trailing-edge blowing. This is quite clear from the leftward movement of the C_L vs α plots without a significant change in the slope (Figs. 7, 8b, and 11). However, now there is a dramatic increase in the $C_{L,\max}$ resulting in significant increase in lift, particularly at lower angles of attack. Obviously, there is considerable room for carefully planned experiments in this area to assess relative performance of the various boundary-layer and circulation control procedures.

Flow Visualization Study

The flow visualization study was carried out in a closed-circuit water channel facility. The model was constructed from Plexiglas, fitted with a leading-edge cylinder, and driven by a compressed-air motor. A suspension of fine aluminum powder was used in conjunction with slit lighting to visualize streaklines. Both angle of attack and cylinder speeds were systematically changed, and still photographs and a video movie were taken.

The study showed, rather dramatically, the effectiveness of this form of boundary-layer control. Presented in Fig. 12 are a few of the steady-state pictures, taken at several angles of attack, with and without the cylinder rotation. In absence of the cylinder rotation, a well-defined separation bubble is quite apparent, particularly at higher angles of attack, with large scale vortices sweeping away downstream. However, with the cylinder rotating at $U_c/U \leq 8$, an essentially attached flow is established over most of the upper surface of the airfoil.

At relatively lower rates of cylinder rotation (say, $U_c/U = 2, 3, 4$), the flow character was found to be similar to that observed at $U_c/U = 0$, with the separation and reattachment regions progressively shifting downstream as the rotation rate increased. This is apparent through the transient flow patterns depicted in Fig. 13, where the cylinder rotation quickly increases from $U_c/U = 0$ to 6.

In fact, the flow pattern was found to be quite unsteady with the vortex layer separating and forming a bubble on reattachment, and the whole structure drifting downstream, diffusing and regrouping at different scales of vortices. Ultimately, the flow sheds large as well as small vortices. Thus, the flow character suggested by the experimentally obtained time-average pressure plots appears to be quite accurate.

Conclusions

The experimental investigation with a symmetrical Joukowsky airfoil using leading- and trailing-edge rotating cylinders brings to light several interesting points of information:

1) In general, rotation of the leading-edge cylinder results in increased suction over the nose. It is the propagation of this lower pressure downstream, however, that determines the effectiveness of the rotation. This depends mainly on the geometry of the nose and smoothness of transition from the cylinder to the airfoil surface. A large gap (> 3mm) substantially decreases beneficial effect of the cylinder rotation.

2) The increased momentum injection into the boundary layer, with an increase in speed of rotation, delays the separation of flow from the upper surface (stall) resulting in a higher $C_{L,\max}$. The existence of a critical speed is also evident beyond which momentum injection through a moving surface appears to have relatively less effect.

3) With the rotation of the leading-edge cylinder, the onset of flow separation occurs at relatively higher angles of attack. The upper surface flow remains attached up to a distance downstream of the leading edge at which point it separates, leading to a large separation bubble, with reattachment towards the trailing edge. The flow, therefore, is not completely separated from the airfoil, thus resulting in a flatter stall peak.

4) The use of a leading-edge cylinder extends the lift curve without substantially changing its slope, thus considerably increasing the maximum lift coefficient and stall angle. The Joukowsky model showed an increase in $C_{L,\max}$ by around 130%, with the stall delayed from 10 to 28 deg.

5) In contrast to the leading-edge cylinder, the use of a trailing-edge cylinder substantially increases the lift before stall. The rotating trailing-edge cylinder acts like a flap shifting the C_L vs α plots to the left. A high rate of rotation of this cylinder results in a dramatic increase in suction, over the airfoil upper surface, thus giving a larger lift. Furthermore, it can be used in conjunction with the leading-edge cylinder, resulting in impressive values of lift over the whole range of low to moderately high angles of incidence ($\alpha \leq 19$ deg). For both the cylinders rotating at $U_c/U = 4$, the $C_{L,\max}$ increased by around 195%, compared to the unmodified base airfoil.

6) The flow visualization study confirmed effectiveness of the concept in a spectacular fashion. It gave better appreciation of the complex flow with a separation bubble and a large turbulent wake. The unsteady flowfield is not stable, but oscillates in the streamwise direction. Furthermore, it substantiated the flow features revealed by the measured pressure profiles in a qualitative fashion.

Acknowledgments

The research project was supported by the Natural Sciences and Engineering Council of Canada, Grant No. A-2181, during the period 1983–1988. The models were fabricated in the Engineering workshop at the University of British Columbia. The assistance of Ed Abell, Senior Technician, in the design and construction of the models is gratefully acknowledged.

References

[1]Goldstein, S., *Modern Development in Fluid Mechanics*, Vols. I and II, Oxford University Press, Oxford, England, 1938.

[2]Lachmann, G. V., *Boundary-layer and Flow Control*, Vols. I and II, Pergamon Press, London, England, 1961.

[3]Rosenhead, L., *Laminar Boundary Layers*, Oxford University Press, Oxford, England, 1966.

[4]Schlichting, H., *Boundary-layer Theory*, McGraw-Hill, New York, 1968.

[5]Chang, P. K., *Separation of Flow*, Pergamon Press, London, England, 1970.

[6]Favre, A., "Contribution a l'Etude Experimentale des Mouvements Hydrodynamiques a Deux Dimensions," Doctoral thesis presented to the Univ. of Paris, 1938.

[7]Alvarez-Calderon, A., and Arnold, F. R., "A Study of the Aerodynamic Characteristics of a High-Lift Device Based on Rotating Cylinder Flap," Stanford Univ. TR RCF-1, 1961.

[8]Brown, D. A., "Peruvians Study Rotating-Cylinder Flap," *Aviation Week and Technology*, Vol. 88, No. 23, Dec. 1964, pp. 70–76.

[9]Cichy, D. R., Harris, J. W., and MacKay, J. K., "Flight Tests of a Rotating Cylinder Flap on a North American Rockwell YOV-10A Aircraft," NASA CR-2135, Nov. 1972.

[10]Weiberg, J. A., Guilianettij, D., Gambucci, G., and Innis, R. C., "Takeoff and Landing Performance and Noise Characteristics of a Deflected STOL Airplane with Interconnected Propellers and Rotating Cylinder Flaps," NASA TM X-62, 320, Dec. 1973.

[11]Cook, W. L., Hickey, D. H., and Quigley, H. C., "Aerodynamics of Jet Flap and Rotating Cylinder Flap STOL Concepts," AGARD Fluid Dynamics Panel on V/STOL Aerodynamics, Paper No. 10. Delft, Netherlands, Apr. 1974.

[12]"Rotating Cylinder Flaps Tested on OV-10A," *Aviation Week and Space Technology*, Vol. 95, No. 16, Oct. 1971, p. 19, and No. 24, Dec. 1971, cover page.

[13]Johnson, W. S., Tennant, J. S., and Stamps, R. E., "Leading-Edge Rotating Cylinder for Boundary-layer Control on Lifting Surfaces," *Journal of Hydrodynautics*, Vol. 9, No. 2, Apr. 1975, pp. 76–78.

[14]Tennant, J. S., Johnson, W. S., and Krothapalli, A., "Rotating Cylinder for Circulation Control on an Airfoil," *Journal of Hydronautics*, Vol. 11, No. 3, July 1976, pp. 102–105.

[15]Tennant, J. S., Johnson, W. S., and Keaton, D. D., "On the Circulation of Boundary layers along Rotating Cylinders," *Journal of Hydronautics*, Vol. 11, No. 2, Apr. 1977, pp. 61–63.

[16]Tennant, J. S., Johnson, W. S., and Keaton, D. D., "Boundary-layer Flow from Fixed to Moving Surfaces including Gap Effects," *Journal of Hydronautics*, Vol. 12, No. 2, Apr. 1978, pp. 81–84.

[17]Modi, V. J., Sun, J. L. C., Akutsu, T., Lake, P., McMillian, K., Swinton, P. G., and Mullins, D., "Moving Surface Boundary-layer Control for Aircraft Operation at High Incidence," *Journal of Aircraft*, Vol. 18, Nov. 1981, pp. 963–968.

[18]Mokhtarian, F., and Modi, V. J., "Fluid Dynamics of Airfoils with Moving Surface Boundary-layer Control," *Journal of Aircraft*, Vol. 25, Feb. 1988, pp. 163–169.